

# KINETIC ANALYSIS OF THERMAL DECOMPOSITION OF SOME Co-COMPLEXES OF THREE UNSYMMETRICAL *Vic*-DIOXIMES LIGANDS

## Model fitting and model-free method

O. Sahin\*, E. Tas and H. Dolas

Department of Chemistry, Harran University, S.Urfa, Turkey

The thermal decomposition of three new reagent cyclohexylamine-*p*-tolylglyoxime (L<sub>1</sub>H<sub>2</sub>), tertiarybutyl amine-*p*-tolylglyoxime (L<sub>2</sub>H<sub>2</sub>) and secondary butylamine-*p*-tolylglyoxime (L<sub>3</sub>H<sub>2</sub>) and their Co-complexes were studied by both isothermal and nonisothermal methods. As expected, the complex structure of Co-complexes, different steps with different activation energies were realized in decomposition process. Model-fitting and model-free kinetic approaches were applied to nonisothermal and isothermal data. The kinetic triplet ( $f(\alpha)$ ,  $A$  and  $E$ ) related to nonisothermal model-fitting method can not be meaningfully compared with values obtained from isothermal method. The complex nature of the multi-step process of the studied compounds was more easily revealed using a wider temperature range in nonisothermal isoconversional method.

**Keywords:** Arrhenius parameter, Co(II) complexes, kinetic analysis, model-fitting and model-free methods, vic-dioxime

### Introduction

The chemistry of oxime/oximato metal complexes has been investigated actively since the time of the first synthesis, e.g. preparation of nickel(II) dimethylglyoximato and recognition of the chelate five-membered character of this complex by Chugaev [1]. Oximes are widely recognized as versatile synthons for a variety of heterocycles [2]. The exceptional stability and unique electronic properties of these complexes can be attributed to their planar structure which is stabilized by hydrogen bonding [3]. When asymmetrical dioximes such as phenylglyoxime or methylglyoxime are employed as starting ligands, a mixture of *fac*- and *mer*-isomers was obtained. However, in some cases one of them was isolated individually [4]. The synthetic chemistry of MN<sub>4</sub> core containing *vic*-dioxime compounds has been described previously [5]. Recently, metal containing oxime complexes are utilized in medicine as well, technetium(V) and copper(II) complexes containing vicinal dioxime currently are used as cerebral and myocardial perfusion imaging agents [6].

### Kinetic computations

The kinetic analysis of solid state decomposition is usually based on a single kinetic equation ( $0 < \alpha < 1$ )

$$\frac{d\alpha}{dt} = k(T)f(\alpha) \quad (1)$$

It is usually assumed that the basic kinetic equation for solid-state decomposition process under non-isothermal condition or in other words the temperature dependence of the rate constant can be expressed as a function of the fractional conversion in the following form [7].

$$\frac{d\alpha}{dt} = A \exp\left(-\frac{E}{RT}\right) f(\alpha) \quad (2)$$

where  $A$  (the pre-exponential factor) and  $E$  (the activation energy) are the Arrhenius parameters and  $R$  is the gas constant. Arrhenius parameters, together with the reaction model are called the kinetic triplet. Since  $\frac{d\alpha}{dt}$  in Eq. (2) can be difficult to measure accurately, temperature dependence in Eq. (2) can be rewritten in the form of:

$$\frac{d\alpha}{dt} = \frac{A}{\beta} \exp\left(-\frac{E}{RT}\right) f(\alpha) \quad (3)$$

where  $\beta = \frac{T - T_0}{t}$  is the heating rate.

By separation of variable and integration, the following equation obtained:

$$g(\alpha) = \int_0^\alpha \frac{d(\alpha)}{f(\alpha)} = \frac{A}{\beta} \int_{T_0}^T \exp\left(-\frac{E}{RT}\right) dT \quad (4)$$

\* Author for correspondence: osahin@harran.edu.tr

For nonisothermal conditions, there are several relationships used to compute Arrhenius parameters each of which is based on an approximate form of the temperature integral [8]. One such approximation is given by Coats-Redfern [9] as following:

$$\ln\left(\frac{g(\alpha)}{T^2}\right) = \ln\left(\frac{AR}{\beta E}\right) \left(1 - \frac{2R\bar{T}}{E}\right) - \frac{E}{RT} \quad (5)$$

where  $\bar{T}$  is the mean experimental temperature. This method is reported [10] to be one of the most frequently used to evaluate nonisothermal data. Arrhenius parameters determined from the plot  $\ln\left(\frac{g(\alpha)}{T^2}\right)$  vs.  $\frac{1}{T}$ . This kind of calculation of kinetic triplet is called as model-fitting method.

Model fitting approach, Arrhenius parameters are found by form of  $g(\alpha)$  assumed. Since in a nonisothermal experiment both  $T$  and  $\alpha$  vary simultaneously, the model-fitting approach generally fail to achieve a clean separation between the temperature dependence  $k(T)$  and the reaction model,  $g(\alpha)$ . For this reason, the model fitting methods tend to procedure highly uncertain value of Arrhenius parameters. The second reason of deviation from model-fitting method between the assumed form of  $g(\alpha)$  and the true reaction model are revealed in decomposition of solid compound having several steps. This means that the effective activation energy determined from thermal analysis experiments will also be a function of temperature and extend of conversion. Thus, the application of model-fitting methods is aimed at extracting a single value of activation energy for an overall process.

The experimental data can be analyzed by other approximation such as temperature integral method, isoconversion method and model free-method [11, 12], since the integral of Eq. (4) in the right-hand side has not exact analytical solution. In all mentioned approximation, the value of integral between 0 and  $T_0$  is negligible, since the starting temperature is near room temperature and the activation energy is not too low. In this case Eq. (4) becomes

$$g(\alpha) = \frac{A}{\beta} \int_0^T \exp\left(-\frac{E}{RT}\right) dT \quad (6)$$

Equation (6) can be rewritten by taking  $x = E/RT$

$$g(\alpha) = \int_0^\alpha \frac{d\alpha}{f(\alpha)} = \frac{AE}{\beta R} \int_x^\infty \frac{\exp(-x)}{x^2} dx = \frac{AE}{\beta R} p(x) \quad (7)$$

The  $p(x)$  function on the right hand side is generally termed as temperature integral [13] which can be approximated in different ways.

The most common of  $p(x)$  function lead to expression of the type

$$p(x) = \frac{\exp(-x)}{x^2} Q(x) \quad (8)$$

where  $Q(x)$  is a function with several particular forms.  $Q(x)$  can be considered the series expansion as given following

$$Q(x) = 1 - 2!\frac{RT}{E} + 3!\left(\frac{RT}{E}\right)^2 - 4!\left(\frac{RT}{E}\right)^3 \dots \quad (9)$$

$Q(x)$  function can also be expressed in the ratio of two fourth order polynomials [14] as given below:

$$Q(x) = \frac{x^4 + 18x^3 + 86x^2 + 96x}{x^4 + 20x^3 + 120x^2 + 240x + 120} \quad (10)$$

All,  $p(x)$ -linear isoconversion methods involve the plotting of  $1/T$  vs. a logarithmic function which depends on the heating rate and temperature. The  $Q(x)$  function shows an approximation for the temperature integral used which is different for the different  $p(x)$ -linear isoconversion methods. Therefore the approximation of the temperature integral is the key to understanding the different methods. The linear isoconversion method equation used in this study can be obtained by combining Eqs (7), (8) at constant fraction transformation as given following

$$g(\alpha) = \frac{ART^2}{\beta E} Q(x) \exp(-x) \quad (11)$$

For constant  $g(\alpha)$ , Eq. (11) becomes

$$\frac{\beta}{T^2 Q(x)} = \frac{AR}{Eg(\alpha)} \exp\left(-\frac{E}{RT}\right) \quad (12)$$

Taking the logarithm of both sides of Eq. (11) gives

$$\ln \frac{\beta}{T^2 Q(x)} = \ln \left( \frac{AR}{Eg(\alpha)} \right) - \frac{E}{RT} \quad (13)$$

In this study, the first three terms in Eq. (9) was considered as  $Q(x)$  function

Iterative procedure is used to approach the exact value of  $E$  in Eq. (12) as following:

- Plotting  $\ln \frac{\beta}{T^2 Q(x)}$  vs.  $\frac{1}{T}$  under the assumption of  $Q(x)=1$  to determine the initial value of  $E_1$ .
- Using  $E_1$  to calculate the value of  $Q(x)$  function, then plotting  $\ln \frac{\beta}{T^2 Q(x)}$  vs.  $\frac{1}{T}$  to calculate a new value of  $E_2$  in slope.

- Comparing step  $E_1$  with  $E_2$ , when  $E_n - E_{n-1} < 0.01 \text{ Kcal mole}^{-1}$ , the last value of  $E_n$  is the exact value of activation energy.

This kind of approximation have been applied by Guan and *et al.* [15]

The present paper is aimed at preparation, characterization and thermal decomposing kinetics based on model-fitting and model free method of three different ligands and their Co complexes.

## Experimental

### Materials

Cyclohexylamine, tertiary butylamine and secondary butylamine (Fluka Chemical Company, Taufkirchen, Germany) and tetra-*n*-butylammonium perchlorate ( $n\text{-Bu}_4\text{NClO}_4$ , Fluka Chemical Company, Taufkirchen, Germany) were used as received.

### Synthesis of the ligands $L_1H_2$ , $L_2H_2$ and $L_3H_2$

*Anti-p*-tolylchloroglyoxime was synthesized as described in the literature [16]. A solution of 15.8 mmol of cyclohexylamine, 15.8 mmol tertiary butylamine and 15.8 mmol secondary butylamine in 30 cm<sup>3</sup> of absolute THF was added to a solution of 15.8 mmol of Et<sub>3</sub>N in 10 cm<sup>3</sup> of absolute THF. This mixture was cooled to -15°C and kept at this temperature, and a solution of 15.8 mmol *anti-p*-tolylchloroglyoxime in 50 cm<sup>3</sup> absolute THF was added dropwise under a N<sub>2</sub> atmosphere with continuous stirring. The addition of the *anti-p*-tolylchloroglyoxime solution was carried out over 1.5 h. The mixture was stirred for 1 h more and the temperature rose to 20°C. Precipitated Et<sub>3</sub>NHCl chloride was filtered and the filtrate was evaporated to remove THF. The oily products were dissolved in 10 cm<sup>3</sup> of CH<sub>2</sub>Cl<sub>2</sub> and 200 cm<sup>3</sup> of *n*-hexane were added to precipitate the compound. This process was then repeated several times. The products were filtered and dried in vacuum.

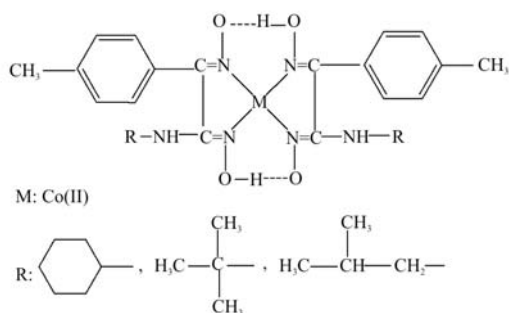


Fig. 1 The structure of the Co(II) complexes

### Synthesis of the cobalt(II) complexes

0.5 mmol  $L_1H_2$ , 0.5 mmol  $L_2H_2$  and 0.5 mmol  $L_3H_2$  was dissolved in EtOH (25 cm<sup>3</sup>). A solution 0.25 mmol of the metal salt [CoCl<sub>2</sub>·6H<sub>2</sub>O] in 10 mL of ethanol was added drop-wise with continuous stirring. The stirred mixture was heated at reflux for 60 min and was maintained at this temperature. The pH of solutions was about 1.5–3.0 and was adjusted to 4.5–5.5 by the addition of a 1% NaOH solution in ethanol. After cooling to room temperature, the complexes were filtered and washed with hot water (3·5 mL). Finally, washed with diethylether and dried at 90°C for 5 h.

The Co-complexes shown in Fig. 1, was prepared by the reaction of cyclohexylamine, tertiary butylamine and secondary butylamine with *anti-p*-tolylchloroglyoxime which was prepared by treating a suspension of *anti-p*-tolylchloroglyoxime in absolute THF with 15.8 mmol in solution of Et<sub>3</sub>N (triethylamine) in absolute THF at -15°C. Excess Et<sub>3</sub>N (triethylamine) was used to neutralize the HCl liberated in the reaction. The ligand has one cyclohexyl ring, one *p*-tolyl group and two oxime groups for  $L_1H_2$ , one *p*-tolyl group, one tertiary group and two oxime groups for  $L_2H_2$  and one *p*-tolyl group, one secondary group and two oxime groups for  $L_3H_2$ , respectively. Mononuclear complexes have been synthesized from  $L_1H_2$ ,  $L_2H_2$  and  $L_3H_2$  with salts of Co(II). Co(II) mononuclear complexes have a metal-ligand ratio of 1:2 and ligands are coordination only by N,N' atoms of vicinal dioximes. In addition to this the cobalt(II) complex has two additional coor-

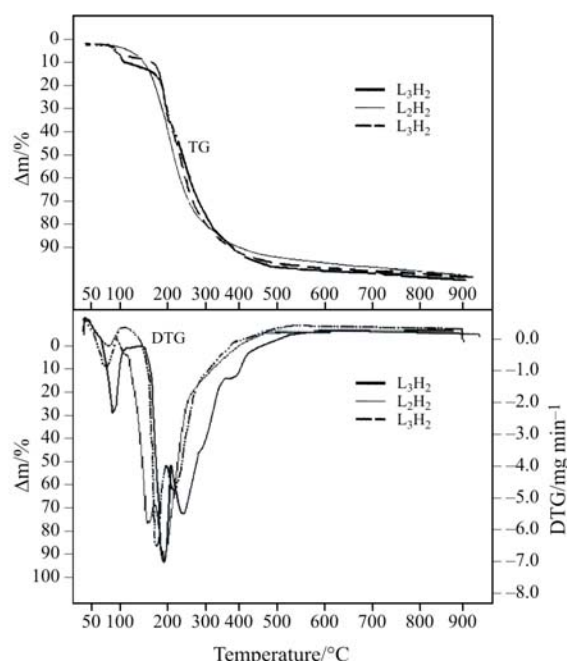
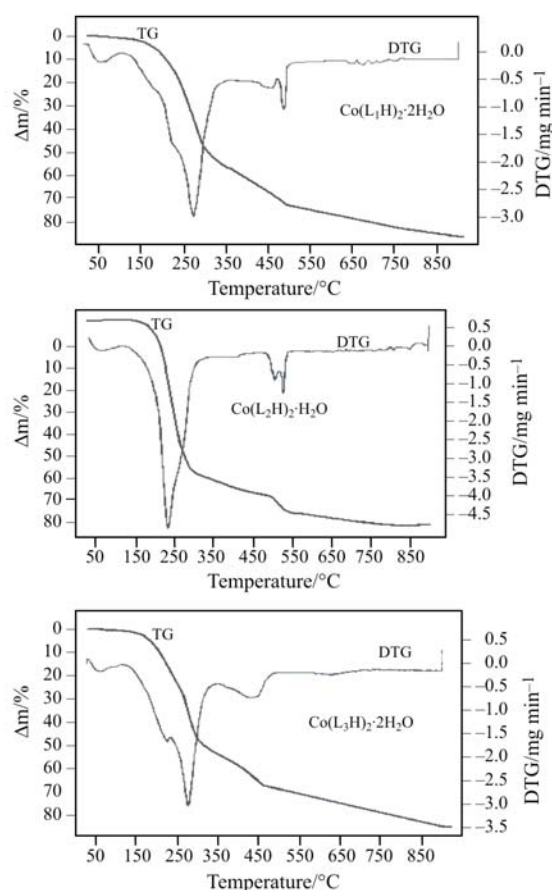


Fig. 2 TG and DTG curves of  $L_{1-3}H_2$  ligands



**Fig. 3** TG and DTG curves of  $\text{Co}(\text{L}_1\text{H})_2 \cdot 2\text{H}_2\text{O}$ ,  $\text{Co}(\text{L}_2\text{H})_2 \cdot 2\text{H}_2\text{O}$  and  $\text{Co}(\text{L}_3\text{H})_2 \cdot 2\text{H}_2\text{O}$

dinated water molecules. Consequently, these *vic*-dioximes is capable of forming mononuclear complexes [17, 18].

### Methods

In experiments, a Setaram TG/DTA/DSC-16 instrument were used for thermal analysis of ligands and their Co complexes. Thermogravimetric tests were performed at nitrogen flow of  $0.850 \text{ mL s}^{-1}$  and at constant heating rates of 5, 10, 15 and  $20^\circ\text{C min}^{-1}$ .

## Results and discussion

The thermal behavior of  $\text{L}_1\text{H}_2$ ,  $\text{L}_2\text{H}_2$ ,  $\text{L}_3\text{H}_2$  and their Co-complexes at heating rate of  $5^\circ\text{C min}^{-1}$  are presented in Figs 2 and 3, respectively. As seen in Figs 2 and 3, each TG curve for both ligands and their Co-complexes, exhibits one and two steps, respectively. However, the DTG curve corresponding to the ligands and for first TG steps of Co-complexes have a clear shoulder. Thus, both thermal decomposition of ligands and the first TG step of Co-complexes corresponding to a complex process consisting in minimum two consecutive or simultaneous reactions. In this work, thermal decomposition of both ligands and the first step of Co-complexes were treated as if they comprised one stage and the kinetic parameters were calculated as for one stage. The character of first step of decomposition of Co-complexes indicates that the process occurs with a narrow range of temperature, in contrast to a second one, which is rather moderate rate in broad temperature. Since  $\text{L}_1\text{H}_2$  and  $\text{L}_3\text{H}_2$  ligands contain the moisture, the thermal decomposition of these ligands appear at two steps each of them ended about  $100^\circ\text{C}$ . The thermal decomposition products, the temperature range concerned and the estimated and the calculated mass loss are listed in Table 1 for both used three ligands and their Co-complexes.

### Nonisothermal study

Inserting various  $g(x)$  models into Eq. (5) results in a set of Arrhenius parameters determined from the plot  $\ln\left(\frac{g(x)}{T^2}\right)$  vs.  $T^{-1}$ . The set of Arrhenius parameters ob-

tained the best four reaction models for the thermal decomposition of both used ligands and their Co-complexes are shown in Tables 2, 3. For each model and heating rate, the goodness of fit is estimated by correlation coefficient,  $r^2$ . The thermal decomposition of used compounds were performed at nonisothermal condition

**Table 1** Mass losses of used ligands and their Co-complexes in different temperature ranges

Compound	Temp. range/ $^\circ\text{C}$	Decomposition product lost	Final product	Mass loss%	
				Found	Calcd.
Ligand, $\text{L}_1\text{H}_2$	55–478	$\text{C}_{15}\text{H}_{21}\text{N}_3\text{O}_2$	–	100	100
$\text{Co}(\text{L}_1\text{H})_2 \cdot 2\text{H}_2\text{O}$	64–342	$\text{C}_{20}\text{H}_{31}\text{O}_3$	$\text{C}_{10}\text{H}_{13}\text{N}_6\text{OCo}$	54.59	54.71
	342–892	$\text{C}_{10}\text{H}_{13}\text{N}_6$	CoO	31.32	33.66
Ligand, $\text{L}_2\text{H}_2$	42–748	$\text{C}_{13}\text{H}_{19}\text{N}_3\text{O}_2$	–	100	100
$\text{Co}(\text{L}_2\text{H})_2 \cdot 2\text{H}_2\text{O}$	152–312	$\text{C}_{22}\text{H}_{40}\text{N}_2\text{O}_2$	$\text{C}_4\text{O}_4\text{N}_4\text{Co}$	61.53	61.59
	312–847	$\text{C}_4\text{N}_4\text{O}_3$	CoO	25.62	25.71
Ligand, $\text{L}_3\text{H}_2$	47–521	$\text{C}_{13}\text{H}_{19}\text{N}_3\text{O}_2$	–	100	100
$\text{Co}(\text{L}_3\text{H})_2 \cdot 2\text{H}_2\text{O}$	59–325	$\text{C}_{19}\text{H}_{29}\text{NO}_2$	$\text{C}_7\text{H}_{11}\text{N}_5\text{O}_4\text{Co}$	51.35	51.27
	325–892	$\text{C}_7\text{H}_{11}\text{N}_5\text{O}_3$	CoO	36.03	36.04

**Table 2** Arrhenius parameters for nonisothermal decomposition of used L<sub>1</sub>H<sub>2</sub>, L<sub>2</sub>H<sub>2</sub> and L<sub>3</sub>H<sub>2</sub> ligands at different heating rates using the Coats-Redfern method

Comp.	Model	Heating rate/°C min <sup>-1</sup>											
		5		10		15		20					
		<i>E</i> /kJ mol <sup>-1</sup>	<i>A</i> /min <sup>-1</sup>	<i>R</i> <sup>2</sup>	<i>E</i> /kJ mol <sup>-1</sup>	<i>A</i> /min <sup>-1</sup>	<i>R</i> <sup>2</sup>	<i>E</i> /kJ mol <sup>-1</sup>	<i>A</i> /min <sup>-1</sup>	<i>R</i> <sup>2</sup>	<i>E</i> /kJ mol <sup>-1</sup>	<i>A</i> /min <sup>-1</sup>	<i>R</i> <sup>2</sup>
L <sub>1</sub> H <sub>2</sub>	<i>n</i> =1	38.6	4.237·10 <sup>2</sup>	0.858	40.7	1.101·10 <sup>3</sup>	0.878	39.3	9.403·10 <sup>2</sup>	0.868	40.5	1.413·10 <sup>3</sup>	0.870
	<i>n</i> =2	59.8	1.665·10 <sup>5</sup>	0.967	62.5	4.380·10 <sup>5</sup>	0.973	60.6	3.059·10 <sup>5</sup>	0.966	62.4	4.857·10 <sup>5</sup>	0.967
	D3	75.2	2.031·10 <sup>5</sup>	0.837	79.1	6.635·10 <sup>5</sup>	0.858	76.8	3.871·10 <sup>5</sup>	0.849	79.0	6.376·10 <sup>5</sup>	0.850
	R3	33.2	2.946·10 <sup>1</sup>	0.797	35.1	7.623·10 <sup>1</sup>	0.822	33.9	6.827·10 <sup>1</sup>	0.810	34.9	1.012·10 <sup>2</sup>	0.812
L <sub>2</sub> H <sub>2</sub>	<i>n</i> =1	22.6	7.451·10 <sup>0</sup>	0.818	18.1	2.795·10 <sup>0</sup>	0.689	—	—	—	26.5	5.870·10 <sup>1</sup>	0.855
	<i>n</i> =2	36.1	6.117·10 <sup>2</sup>	0.953	38.7	1.651·10 <sup>3</sup>	0.928	—	—	—	38.1	2.047·10 <sup>3</sup>	0.957
	D3	46.7	2.485·10 <sup>2</sup>	0.823	39.1	3.458·10 <sup>1</sup>	0.728	—	—	—	41.8	1.036·10 <sup>2</sup>	0.793
	D4	42.5	6.574·10 <sup>1</sup>	0.787	35.3	1.038·10 <sup>1</sup>	0.683	—	—	—	37.9	3.131·10 <sup>1</sup>	0.750
L <sub>3</sub> H <sub>2</sub>	<i>n</i> =1	24.5	1.319·10 <sup>1</sup>	0.904	26.0	3.028·10 <sup>1</sup>	0.901	26.5	3.812·10 <sup>1</sup>	0.774	31.6	1.893·10 <sup>2</sup>	0.888
	<i>n</i> =2	35.3	4.705·10 <sup>2</sup>	0.941	37.8	1.243·10 <sup>3</sup>	0.957	40.0	2.126·10 <sup>3</sup>	0.921	46.3	1.335·10 <sup>4</sup>	0.978
	D3	51.1	8.393·10 <sup>2</sup>	0.911	54.1	2.144·10 <sup>3</sup>	0.903	54.7	2.196·10 <sup>3</sup>	0.790	64.3	2.893·10 <sup>4</sup>	0.881
	D4	47.6	2.695·10 <sup>2</sup>	0.894	50.2	6.595·10 <sup>2</sup>	0.882	50.3	6.153·10 <sup>2</sup>	0.755	59.6	7.476·10 <sup>3</sup>	0.853

**Table 3** Arrhenius parameters for nonisothermal decomposition of used  $\text{Co}(\text{L}_1\text{H})_2 \cdot 2\text{H}_2\text{O}$ ,  $\text{Co}(\text{L}_2\text{H})_2 \cdot 2\text{H}_2\text{O}$  and  $\text{Co}(\text{L}_3\text{H})_2 \cdot 2\text{H}_2\text{O}$  complexes at different heating rate using the Coats-Redfern method

Compound	Model	Heating rate/ $^{\circ}\text{C min}^{-1}$											
		5		10		15		20					
		$E/\text{kJ mol}^{-1}$	$A/\text{min}^{-1}$	$R^2$	$E/\text{kJ mol}^{-1}$	$A/\text{min}^{-1}$	$R^2$	$E/\text{kJ mol}^{-1}$	$A/\text{min}^{-1}$	$R^2$	$E/\text{kJ mol}^{-1}$	$A/\text{min}^{-1}$	$R^2$
$\text{Co}(\text{L}_1\text{H})_2 \cdot 2\text{H}_2\text{O}$ I step	$n=1$	30.1	$2.451 \cdot 10^1$	0.962	$1.275 \cdot 10^2$	0.982	32.1	$8.976 \cdot 10^1$	0.936	37.2	$3.634 \cdot 10^2$	0.966	
	$n=2/3$	27.9	$1.207 \cdot 10^1$	0.952	$5.873 \cdot 10^1$	0.968	29.6	$4.074 \cdot 10^1$	0.906	34.4	$1.573 \cdot 10^2$	0.942	
	D3	63.7	$3.796 \cdot 10^3$	0.964	$4.1780 \cdot 10^4$	0.977	67.8	$1.643 \cdot 10^4$	0.934	77.5	$1.576 \cdot 10^5$	0.958	
	R3	27.9	$4.024 \cdot 10^0$	0.952	$1.957 \cdot 10^1$	0.968	29.6	$1.357 \cdot 10^1$	0.906	34.4	$5.246 \cdot 10^1$	0.942	
$\text{Co}(\text{L}_1\text{H})_2 \cdot 2\text{H}_2\text{O}$ II step	$n=1$	86.1	$2.297 \cdot 10^4$	0.827	$1.133 \cdot 10^3$	0.819	65.2	$1.023 \cdot 10^3$	0.823	55.2	$1.005 \cdot 10^2$	0.891	
	$n=2$	132.7	$7.222 \cdot 10^7$	0.952	$5.277 \cdot 10^5$	0.908	100.0	$3.847 \cdot 10^5$	0.912	84.7	$1.156 \cdot 10^4$	0.948	
	D3	162.2	$2.139 \cdot 10^8$	0.799	$9.243 \cdot 10^5$	0.805	126.7	$5.964 \cdot 10^5$	0.810	110.9	$1.183 \cdot 10^4$	0.882	
	R3	74.3	$9.450 \cdot 10^2$	0.767	$7.368 \cdot 10^1$	0.765	56.3	$7.021 \cdot 10^1$	0.769	47.6	$9.319 \cdot 10^0$	0.842	
$\text{Co}(\text{L}_2\text{H})_2 \cdot 2\text{H}_2\text{O}$ I step	$n=1$	58.6	$4.775 \cdot 10^4$	0.900	$1.786 \cdot 10^5$	0.896	58.1	$9.095 \cdot 10^4$	0.845	66.3	$8.467 \cdot 10^5$	0.865	
	$n=2$	88.0	$1.064 \cdot 10^8$	0.979	$5.204 \cdot 10^8$	0.976	101.7	$5.592 \cdot 10^9$	0.984	94.9	$1.249 \cdot 10^9$	0.949	
	D3	111.2	$6.717 \cdot 10^8$	0.877	$3.973 \cdot 10^9$	0.874	11.4	$8.134 \cdot 10^{-1}$	0.822	126.6	$5.274 \cdot 10^1$	0.847	
	A2	24.9	$1.001 \cdot 10^1$	0.862	$3.360 \cdot 10^1$	0.859	31.7	$1.887 \cdot 10^2$	0.904	28.6	$1.073 \cdot 10^2$	0.823	
$\text{Co}(\text{L}_2\text{H})_2 \cdot 2\text{H}_2\text{O}$ II step	$n=1$	114.1	$4.718 \cdot 10^6$	0.932	$1.257 \cdot 10^7$	0.903	126.1	$3.431 \cdot 10^7$	0.898	96.8	$2.423 \cdot 10^5$	0.833	
	$n=2$	160.1	$1.732 \cdot 10^{10}$	0.930	$9.761 \cdot 10^{10}$	0.971	181.6	$3.659 \cdot 10^{11}$	0.973	142.7	$5.007 \cdot 10^8$	0.938	
	D3	218.1	$5.983 \cdot 10^{12}$	0.922	$1.282 \cdot 10^{13}$	0.879	237.3	$5.418 \cdot 10^{13}$	0.873	184.0	$6.667 \cdot 10^9$	0.808	
	A2	50.8	$1.244 \cdot 10^2$	0.916	$2.787 \cdot 10^2$	0.878	56.4	$5.706 \cdot 10^2$	0.873	41.4	$4.450 \cdot 10^1$	0.781	
$\text{Co}(\text{L}_3\text{H})_2 \cdot 2\text{H}_2\text{O}$ I step	$n=0$	37.1	$2.0406 \cdot 10^2$	0.991	$8.599 \cdot 10^2$	0.978	43.2	$1.951 \cdot 10^3$	0.985	44.8	$3.132 \cdot 10^3$	0.986	
	$n=2/3$	46.3	$3.029 \cdot 10^3$	0.993	$1.579 \cdot 10^4$	0.993	89.7	$5.271 \cdot 10^8$	0.895	55.9	$6.211 \cdot 10^4$	0.994	
	R2	43.7	$7.042 \cdot 10^2$	0.996	$3.449 \cdot 10^3$	0.993	50.9	$8.116 \cdot 10^3$	0.995	52.7	$1.327 \cdot 10^4$	0.995	
	D4	93.6	$1.929 \cdot 10^7$	0.996	$2.104 \cdot 10^8$	0.993	108.0	$7.467 \cdot 10^8$	0.996	111.7	$1.480 \cdot 10^9$	0.996	
$\text{Co}(\text{L}_3\text{H})_2 \cdot 2\text{H}_2\text{O}$ II step	$n=1$	26.3	$1.346 \cdot 10^0$	0.825	$4.019 \cdot 10^0$	0.783	28.0	$4.966 \cdot 10^8$	0.805	24.6	$2.804 \cdot 10^0$	0.759	
	$n=2$	49.3	$1.851 \cdot 10^2$	0.943	$3.065 \cdot 10^2$	0.944	48.7	$4.202 \cdot 10^2$	0.955	47.9	$3.515 \cdot 10^2$	0.937	
	$n=2/3$	20.7	$3.605 \cdot 10^{-1}$	0.717	$9.134 \cdot 10^{-1}$	0.678	22.7	$1.527 \cdot 10^0$	0.708	20.4	$1.042 \cdot 10^0$	0.633	
	D3	54.4	$1.425 \cdot 10^1$	0.824	$3.299 \cdot 10^1$	0.799	58.4	$7.661 \cdot 10^1$	0.811	54.5	$3.430 \cdot 10^1$	0.767	

at constant heating rate of 5, 10, 15 and 20°C min<sup>-1</sup>, since a single step of nonisothermal ( $\alpha$ ,  $T$ ,  $t$ ) data give similarly satisfactory fits to most of many equations. This set is conventionally taken as the group of kinetic models that are characteristic of decomposition reaction of solid. The apparent magnitude of the Arrhenius parameters, however vary significantly with each alternative kinetic model compared [19].

As seen in Table 2, the nonisothermal kinetic parameters obtained by CR method for L<sub>1</sub>H<sub>2</sub>, L<sub>2</sub>H<sub>2</sub> and L<sub>3</sub>H<sub>2</sub> ligands can be represented by four different kinetic models with respect to  $r^2$  values, but the apparent activation energy is far from each other for each ligand. In this case, there is no adequate criterion for distinguishing the best set of kinetic parameters at nonisothermal condition. Also, in Table 3, the thermal decomposition steps of Co-complexes are represented by four different models. The difference between  $r^2$  values is very small, but the apparent activation energy values changes by a factor  $\times 2$  or more. This kind of result has been given in literature by Vyazovkin [20]. The general result for data given in Tables 2, 3 obtained by CR method can be summarized as following

- CR approach to kinetic analysis is generally unsuitable for determination of kinetic triplex.
- The interrelationship between the exponent  $n$  and activation energy found by CR method in Table 3 is effectively unable to separate the individual contributions to the composite function.

*Isothermal study*

Rearrangement and integration of Eq. (1) for isothermal condition gives

$$g_i(\alpha) = \int_0^\alpha \frac{d\alpha}{f(\alpha)} = k_i(T)t \quad (14)$$

The subscript  $i$  has been introduced to emphasize that substituting a particular reaction model into Eq. (14) results in calculation the suitable rate constant determined from the slope of a plot of  $g(\alpha)$  vs.  $t$ . In this study, the statistical equivalent kinetic triplets determined from nonisothermal data using the model fitting method have been used to determine isothermal data [21] as follow:

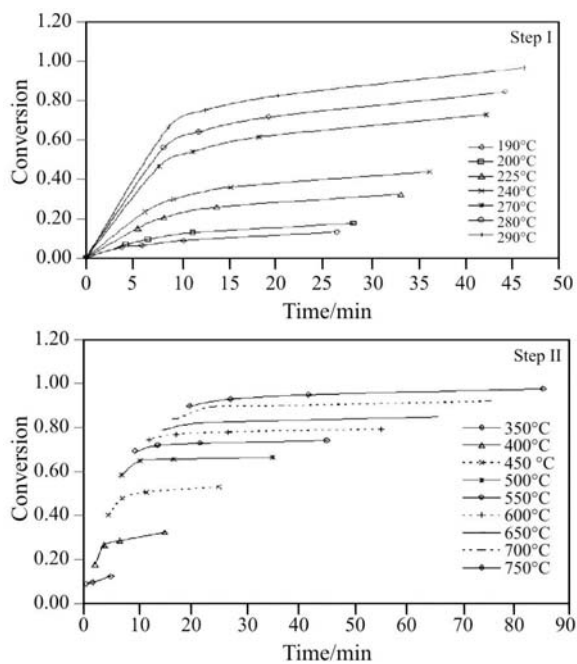


Fig. 4 Prediction of isothermal decomposition data of Co(L<sub>3</sub>H)<sub>2</sub>·2H<sub>2</sub>O for both Step I and Step II from nonisothermal TG curves

$$k_i = Ae^{-\frac{E}{RT_i}} = \frac{g(\alpha)}{t_\alpha} \quad (15)$$

where  $t_\alpha$  is the time to reach the extent of conversion  $\alpha$  at the constant temperature of  $T_i$ .

Figure 4 represents the isothermal decomposition data obtained from nonisothermal TG curves for Co(L<sub>3</sub>H)<sub>2</sub>·2H<sub>2</sub>O complex. As can be seen in Fig. 4, the changes of conversion with time is nearly parallel for both decomposition steps of Co(L<sub>3</sub>H)<sub>2</sub>·2H<sub>2</sub>O separately.

For different reaction model, the rate constants are evaluated at several temperatures as given in Eq. (14), the Arrhenius parameters are determined by using the Arrhenius equation in its logarithmic form,

$$\ln(k_i) = \ln(A) - \frac{E_i}{RT_i} \quad (16)$$

Figure 5 depicts a plot of  $\ln(k)$  vs.  $1/T$ . Arrhenius parameters found for the isothermal decomposition of used Co-Complexes by the model fitting method are illustrated in Table 4. It is believed that the analysis of

Table 4 Arrhenius parameters for isothermal decomposition of used Co-complexes determined using the model-fitting method

Compound	Model	$E/kJ\ mol^{-1}$	$A/min^{-1}$	$R^2$
Co(L <sub>1</sub> H) <sub>2</sub> ·2H <sub>2</sub> O	I step	43.7	13.681	0.983
	II step	$n=1$	42.3	15.799
Co(L <sub>2</sub> H) <sub>2</sub> ·2H <sub>2</sub> O	I step	46.7	114.663	0.982
	II step	$n=2$	105.6	51149.535
Co(L <sub>3</sub> H) <sub>2</sub> ·2H <sub>2</sub> O	I step	77.1	178974.748	0.999
	II step	$n=1$	119.7	255505.701

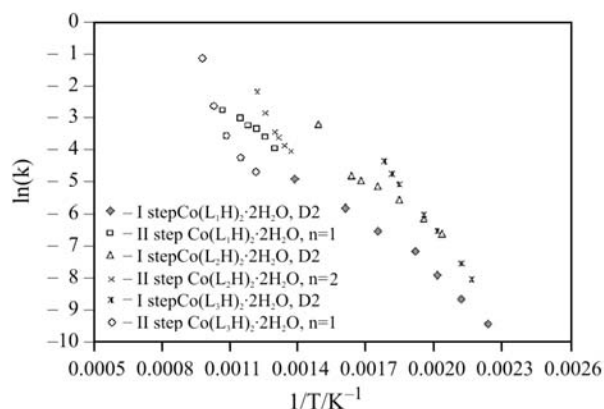


**Fig. 5** Arrhenius plots of the thermal decomposition of Co-complexes

isothermal kinetic parameters is more reliable, since the temperature is held constant during experiments. Therefore, the results of nonisothermal experiments are expected to agree with isothermal data. As seen in Table 4, the activation energy values obtained by isothermal methods and the best model represented thermal decomposition of the Co-complexes data are very differ from that is obtained from nonisothermal method. This inaccuracy between two methods was explained in nonisothermal study section. On the other hand, it must be taken into account that in the isothermal condition the reaction are very slow at the low temperature, so that the experiments will be limited by long terms, while for high temperature the reaction will be too fast. As a result of this restriction, it can be said that the isothermal experimental is limited by temperature.

#### Model-free linear isoconversional method study

Model fitting methods are designed to extract a single step of global Arrhenius parameters for the whole process and are therefore unable to reveal this type of complexity in solid state reactions. The values obtained in such a way are averages that do not reflect changes in the mechanism and kinetics with the temperature and extend of conversion. The model-free isoconversional method allows for unmistakable detecting multi-stage kinetics as dependence of the activation energy on the extend of conversion. Furthermore, it was shown that revealing the dependence of the activation energy on the conversion not only helps to disclose the complexity of a process, but also helps to identify its kinetics scheme. Thus, it is possible to obtain information about the mechanism of a process and predict its kinetic without the knowledge of both the reaction model and the pre-exponential factor.

For a set of experiments conducted at different heating rates, the activation energy can be calculated at any particular value of  $\alpha$  in Eq. (13). The best value of

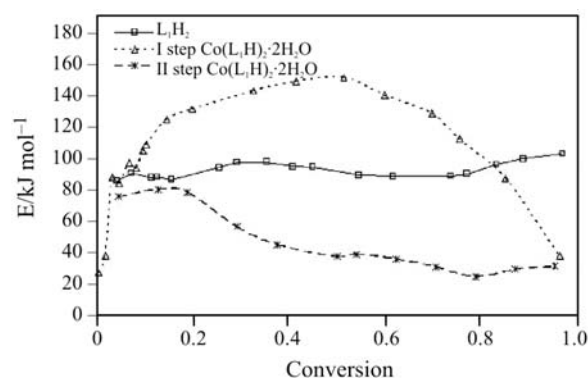


**Fig. 6** Dependence of the activation energy of  $L_1H_2$  ligand and their  $Co(L_1H_2)_2 \cdot 2H_2O$  complex conversion determined using the model-free isoconversional method for the nonisothermal data

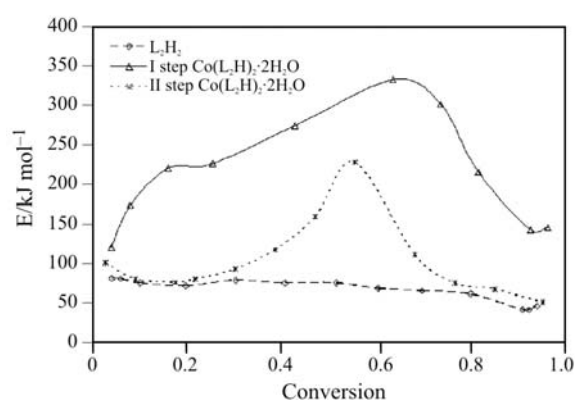


**Fig. 7** Dependence of the activation energy of  $L_2H_2$  ligand and their  $Co(L_2H_2)_2 \cdot 2H_2O$  complex conversion determined using the model-free isoconversional method for the nonisothermal data

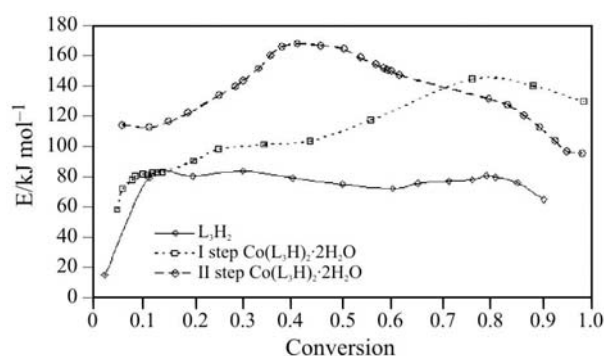


**Fig. 8** Dependence of the activation energy of  $L_3H_2$  ligand and their  $Co(L_3H_2)_2 \cdot 2H_2O$  complex conversion determined using the model-free isoconversional method for the nonisothermal data

activation energy,  $E$  is found for each value of conversion ( $\alpha$ ), in order to find the dependence of the activation energy on the extent of conversion. Figures 6–8 show the activation energy dependencies determined for the nonisothermal decomposition of  $L_1H_2$ ,  $L_2H_2$  and  $L_3H_2$  ligands and their Co-complexes.



As shown in Figs 6–8, the value of the activation energy increases or decreases with the degree of conversion for used complexes. Variation in the value of activation energy may be a hint of change in reaction mechanism with reaction progressing in some cases. If activation energy values are not constant with conversion for any decomposition, then one is probably dealing with either a change in mechanism as the reaction proceeds or a more complex situation such as a mutually independent multiple, competitive or consecutive reaction system, reversible reaction [22–25].

First step of the nonisothermal decomposition of  $\text{Co}(\text{L}_1\text{H})_2 \cdot 2\text{H}_2\text{O}$  complex gives an  $E$ – $\alpha$  dependence (Fig. 6) that rises from about  $140 \text{ kJ mol}^{-1}$  at  $\alpha=0.4$  and decrease at high conversion to nearly  $40 \text{ kJ mol}^{-1}$ . For second step of same Co-complex, the activation energy decreases monotonically to  $40 \text{ kJ mol}^{-1}$  near the end of reaction.

For the nonisothermal decomposition of  $\text{Co}(\text{L}_2\text{H})_2 \cdot 2\text{H}_2\text{O}$  complex, the changes in the activation energy (Fig. 7) for both steps increase with increasing conversion and reached a maximum around 325 and  $200 \text{ kJ mol}^{-1}$  at around  $\alpha=0.6$  and  $\alpha=0.5$  then decrease to about 150 and  $50 \text{ kJ mol}^{-1}$  near the end of reaction, for the second and first step, respectively. Figure 8 also shows the  $E$ – $\alpha$  dependence for the nonisothermal decomposition of  $\text{Co}(\text{L}_3\text{H})_2 \cdot 2\text{H}_2\text{O}$  complexes, as computed by the linear isoconversional method. The activation energy increases to maximum around 145,  $170 \text{ kJ mol}^{-1}$  at  $\alpha=0.77$  and  $\alpha=0.4$  and then decrease 130 and  $92 \text{ kJ mol}^{-1}$  near the complexation of the reaction for first and second step of  $\text{Co}(\text{L}_1\text{H})_2 \cdot 2\text{H}_2\text{O}$  complexes, respectively. For three of used ligands, the change of activation energy with conversion,  $\alpha$  is approximately constant.

## Conclusions

The application of the model fitting method to a multi-step decomposition of  $\text{Co}(\text{L}_1\text{H})_2 \cdot 2\text{H}_2\text{O}$ ,  $\text{Co}(\text{L}_2\text{H})_2 \cdot 2\text{H}_2\text{O}$  and  $\text{Co}(\text{L}_3\text{H})_2 \cdot 2\text{H}_2\text{O}$  complexes results to be unsuitable for the nonisothermal data. For isothermal data model-fitting method gives rise to apparently reliable results that are likely to conceal the kinetic complexity. A variable alternative to the model-fitting method is the model-free isoconversional method. By this method nonisothermal data can be easily be analyzed and the activation energy,  $E$  vs. conversion,  $\alpha$  plots can reveal complexities in the reaction kinetics. The thermal decomposition of  $\text{L}_1\text{H}_2$ ,  $\text{L}_2\text{H}_2$  and  $\text{L}_3\text{H}_2$  ligands and their Co-complexes was carried out by the general known method named model fitting and isoconversional method to determine the Arrhenius kinetic parameters and the

reaction mechanism. The obtained activation energies values for  $\text{L}_1\text{H}_2$ ,  $\text{L}_2\text{H}_2$  and  $\text{L}_3\text{H}_2$  ligands are approximately constant, since decomposition of used ligands realized at single step.

## References

- 1 L. A. Chugaev, Zh. Russ. Physicochem. Soc., 41 (1909) 184.
- 2 V. Y. Kukushkin, D. Tudela and A. J. L. Pombeiro, Coord. Chem. Rev., 156 (1996) 333.
- 3 B. G. Brown, Prog. Inorg. Chem., 18 (1973) 17.
- 4 V. E. Zavodnik, V. K. Belsky, Y. Z. Voloshin and O. A. Varzatsky, J. Coord. Chem., 23 (1993) 97.
- 5 Y. Gok, S. Z. Yıldız and M. Tüfekçi, J. Coord. Chem., 12 (1993) 2097.
- 6 M. J. Prushan, A. W. Addison and R. J. Butcher, Inorg. Chem. Acta, 300-302 (2000) 992.
- 7 G. O. Piloyan, I. D. Ryabchikov and O. S. Novikova, Nature, 212 (1966) 1229.
- 8 M. E. Brown, D. Dollimore and A. K. Galwey, Reaction in the Solid State Comprehensive Chemical Kinetic, Vol. 22, Elsevier, Amsterdam, 1980.
- 9 A. W. Coats and J. P. Redfern, Nature, 201 (1964) 68.
- 10 N. J. Carr and A. K. Galwey, Thermochim. Acta, 79 (1984) 323.
- 11 J. A. F. R. Rodrigues, D. F. Parra and A. B. Lugão, J. Therm. Anal. Cal., 79 (2005) 379.
- 12 A. Cadenato, J. M. Morancho, X. Fernández-Francos, J. M. Salla and X. Ramis, J. Therm. Anal. Cal., OnlineFirst: DOI: 10.1007/s10973-006-7567-5).
- 13 G. H. Heal, Thermochim. Acta, 340/341 (1999) 69.
- 14 G. I. Senum and R. T. Yang, J. Thermal Anal., 16 (1977) 1033.
- 15 C. Guan, L. Li, D. Chen, Z. Gao and W. Sun, Thermochim. Acta, 413 (2004) 31.
- 16 H. Britzingen and R. Titzmann, Ber. Dtsch. Chem. Ges., 85 (1952) 345.
- 17 D. Dolphin, B12, Vol.1 and Vol 2, Wiley, New York, (1982).
- 18 E. Hamuryudan and Ö. Bekaroğlu, Chem. Ber., 127 (1994) 2483.
- 19 J. M. Criado and A. Ortega, J. Thermal Anal., 29 (1984) 1225.
- 20 S. Vyazovkin, J. Therm. Anal. Cal., 64 (2001) 829.
- 21 S. Vyazovkin and C. A. Wight, Thermochim. Acta, 340-341 (1999) 53.
- 22 S. Vyazovkin and A. I. Lesnikovich, Thermochim. Acta, 165 (1990) 273.
- 23 S. Vyazovkin, V. I. Goryachko and A. I. Lesnikovich, Thermochim. Acta, 197 (1992) 41.
- 24 S. Vyazovkin and W. Linert, J. Chem. Kinet., 27 (1995) 73.
- 25 S. Vyazovkin, J. Therm. Anal. Cal., 83 (2006) 45.

Received: March 25, 2005

Accepted: December 28, 2006

OnlineFirst: April 29, 2007

DOI: 10.1007/s10973-005-7019-7